

## Lattice Dynamics of Alkali Halides

A. N. Basu

*Physics Department, Jadavpur University, Calcutta-32, India*

S. Sengupta

*Physics Department, Maulana Azad College, Calcutta-13, India*

(Received 11 September 1972)

The deformable-shell model developed by Basu and Sengupta and later substantiated by a potential form by Sarkar and Sengupta has found wide application in describing the different static properties of ionic crystals of both NaCl and CsCl structures. But so far a complete calculation of the dynamical properties of ionic crystals has been reported for only one crystal. Further, from a critical comparison of the different lattice-dynamical models which effectively introduce many-body interactions between the ions, we have found that there are certain differences between them, some of which are quite fundamental in nature. Moreover, of the current phenomenological models, the deformable-shell model alone is capable of reasonably treating both the static and the dynamic properties of the crystals. Hence it is important to know the results of the calculation according to different models. In this work we present the lattice-dynamic calculation on the following five crystals, NaCl, NaBr, KI, KCl, and KBr according to the deformable-shell model. In order to obtain the parameters, the well-known macroscopic quantities have been used and no least-square-fitting procedure has been adopted. The parameters obtained from the theory have been used to calculate the phonon dispersion relation in both the symmetry and the off-symmetry directions (where experimental results are available) and the variation of the Debye temperature from the frequency spectra for these crystals. We have consistently used the polarizable negative-ion model for all of them. The results thus obtained agree well with experiment. Other theoretical-model results are also discussed in detail.

### I. INTRODUCTION

The shell model describing the lattice dynamics of alkali halides has been improved by the inclusion of effective many-body interactions between the particle of the ionic lattice. Among such improved models are the "breathing"-shell model (BSM) by Schröder,<sup>1</sup> the three-body-interaction model proposed by Lundqvist<sup>2</sup> and applied by Singh and Verma,<sup>3</sup> and the deformable-shell model (DSM) by Basu and Sengupta.<sup>4</sup> In a recent investigation<sup>5</sup> we have seen that, despite the apparent similarity in the formal structure of the dynamical equations of these models, there are fundamental differences between them. From a critical comparison of the above-mentioned models it is concluded that they differ not only with respect to the physical content but also that they imply different types of constraint on the system. Moreover, while calculating the static properties such as the cohesive energy, the relative stability, the phase-transition pressure, or the anharmonic properties such as variation of bulk modulus with temperature and pressure, thermal expansion of solid, etc., all these models lead to different results. Sarkar and Sengupta<sup>6</sup> and Sarkar<sup>7</sup> have successfully applied the deformable-shell model to study these properties of ionic crystals. But both the breathing-shell model and the Lundqvist model lead to difficulties in interpreting these properties. For example, Lundqvist's three-body interaction in relation to the relative stability of crystal structures

shows a strong preference for CsCl structure,<sup>8</sup> and the breathing-shell model in relation to the change in ionic radius of an ion when put in a crystal lattice leads to a result<sup>5</sup> contrary to observation. No such anomaly has yet been found with the deformable-shell model.

We have further noticed while calculating the dielectric properties<sup>9</sup> of the ionic crystal that both the polarization mechanism of an ion and the type of many-body interaction implied in the different models do not lead to identical results. Hence at this stage in order to realize the validity of any model we must have the results of calculation of the different properties of a crystal by a single model. Both the breathing-shell model and the Lundqvist model have been exhaustively exploited to study the lattice dynamics of alkali halides, but only a few attempts have been made to apply them to study the lattice statics of alkali halides. The contrary is true for the deformable-shell model. Hence in this paper we propose to apply the deformable-shell model to study the lattice dynamics of alkali halides.

### II. MODEL AND CALCULATION

We present here a short account of the deformable-shell model (DSM). The details are given in Basu and Sengupta<sup>4</sup> and Sarkar and Sengupta.<sup>6</sup>

The distribution of the electron charge cloud around each nucleus will in general depend upon the relative position of different ions in the crystal. The equilibrium density will be altered when the

ions are displaced from their equilibrium position. The deformation of the charge cloud may be expanded in terms of spherical harmonics of different orders.<sup>10</sup> The zero-order term gives rise to an isotropic scalar deformation, the first-order term to a dipole deformation, the second-order term to a quadrupole deformation, and so on. In the DSM, the first two terms are taken into account. The shell model<sup>11</sup> is used to include the effect of the dipole deformation. For simplification, the scalar deformation is represented by a single parameter. The energy of deformation may be expanded in powers of this deformation parameter. It is further assumed that the deformation parameter for a particular ion is proportional to the radial component of the overlap force exerted on the ion by its nearest neighbors. With this assumption we can express the deformation energy as a function of the displacement of the ions from their equilibrium position. If  $\tilde{u}(l, k)$  is the displacement of the  $lk$  ion, then the expression for the deformation energy may be written as

$$E_d = \frac{1}{2} \sum_{l'k', l''k''} \Phi^{(d)} \left( \begin{matrix} l' & l'' \\ k' & k'' \end{matrix} \right) \tilde{u} \left( \begin{matrix} l' \\ k' \end{matrix} \right) \tilde{u} \left( \begin{matrix} l'' \\ k'' \end{matrix} \right), \quad (1)$$

where the force constant tensor  $\Phi^{(d)}$  for the deformation energy for crystals with a center of symmetry is given by

$$\Phi^{(d)} \left( \begin{matrix} l' & l'' \\ k' & k'' \end{matrix} \right) = \sum_{lk(\text{cnn})} C(k) [\phi''(\gamma)]^2 \bar{\Gamma} \left( \begin{matrix} l & l' \\ k & k' \end{matrix} \right) \bar{\Gamma} \left( \begin{matrix} l & l'' \\ k & k'' \end{matrix} \right), \quad (1')$$

where the constant  $C(k)$  is a measure of the deformability of the  $k$ th ion,  $\phi(\gamma)$  is the two-body central-overlap interaction, and  $\bar{\Gamma}(ll', kk')$  is the equilibrium separation between the  $lk$  and  $l'k'$  particles. The summation over  $lk$  runs over all the common nearest neighbors (cnn) of  $l'k'$  and  $l''k''$  ions. It is evident from Eq. (1') that the deformation force constant has a three-body character. It may also be noted that the scalar deformation introduces extra force constant between like-particle second neighbors only.

To introduce the effect of deformability within the framework of the shell model, we divide each ion  $k$  of charge  $Z_k$  into a core of charge  $Z_k + Y_k$  and a shell of charge  $-Y_k$ . We put  $k=1, 2$ , to indicate the cores of the positive and the negative ions, respectively, and  $k=3, 4$ , for the corresponding shells. Assuming that overlap interaction acts entirely through the shells, the deformation force constant in Eq. (1') will introduce extra interaction between the shells (3, 3) and (4, 4) and the corresponding contribution to the dynamical matrix is designated as  $\underline{M}^{(d)}(3, 3)$  and  $\underline{M}^{(d)}(4, 4)$ . Let  $\underline{U}(1)$  and  $\underline{U}(2)$  be the amplitude vectors for the core displacements of positive and negative

ions, respectively, and the shell-core separation vectors for the corresponding ions be  $\underline{W}_1$  and  $\underline{W}_2$ . Then the dynamical equations for determining the frequency  $\omega$  of the system may be written in the form

$$(\underline{R} + \underline{D}_0 + \underline{Z} \underline{C} \underline{Z}) \underline{U} + (\underline{R} + \underline{D}_0 - \underline{Z} \underline{C} \underline{Y}) \underline{W} = m\omega^2 \underline{U}, \quad (2)$$

$$(\underline{R}^T + \underline{D}_0^T - \underline{Y} \underline{C} \underline{Z}) \underline{U} + (\underline{K} + \underline{R} + \underline{D}_0 + \underline{Y} \underline{C} \underline{Y}) \underline{W} = 0,$$

where  $\underline{Z}$ ,  $\underline{Y}$ ,  $\underline{m}$  are  $6 \times 6$  diagonal matrices for the ionic charge, shell charge, and mass of the ions,  $\underline{U} = \underline{U}_1, \underline{U}_2$  and  $\underline{W} = (\underline{W}_1, \underline{W}_2)$  are six-dimensional vectors, and  $\underline{R}$ ,  $\underline{C}$ ,  $\underline{K}$  are  $6 \times 6$  dynamical matrices corresponding to the overlap interaction, Coulomb interaction, and core-shell spring interaction, respectively, and  $\underline{D}_0$  is the real  $6 \times 6$  dynamical matrix corresponding to the extra interaction due to deformation and is given by

$$\underline{D}_0 = \begin{bmatrix} \underline{M}^{(d)}(33) & 0 \\ 0 & \underline{M}^{(d)}(44) \end{bmatrix}. \quad (3)$$

It may be noted that  $\underline{D}_0$  is a real self-adjoint matrix.

In application we have considered only the negative ion to be polarizable. Setting  $Z$  (the ionic charge) equal to unity, then the total number of parameters retained is six; they are,  $\phi''$ ,  $\phi'/r_0$  (nearest-neighbor force constants),  $P(1)$ ,  $P(2)$ , [deformability parameters,  $P(k) = C(k)\phi'^2 r_0^2$ ],  $Y$  (negative-ion shell charge), and  $K$  (core-shell spring constant). The parameters,  $\phi''$ ,  $\phi'/r_0$ , and [ $P(1) + P(2)$ ] are determined from the elastic constants obtained from the following expression<sup>12</sup> by the long-wave (LW) method:

$$e_{ijkl}^{LW} = \bar{C}_{ijkl}(\text{expt.}) + \frac{d\bar{C}_{ijkl}}{dp} (P - P_0) - P(\delta_{ij}\delta_{ik} + \delta_{ij}\delta_{jk} - \delta_{ij}\delta_{kl}), \quad (4)$$

where  $\bar{C}$  is the harmonic value of the elastic constant,  $2r_0$  is the lattice constant at the temperature at which the normal mode frequencies are to be calculated,  $P_0$  is the atmospheric pressure, and

$$P - P_0 = (\bar{C}_{11} + 2\bar{C}_{12}) \frac{\tilde{r}_0 - r_0}{r_0}. \quad (5)$$

The necessity of using the elastic constants obtained from the long-wave theory as outlined above has been discussed in detail by Roy *et al.*<sup>12</sup>  $Y$ ,  $K$ , and  $P(1)$  are determined from the dielectric constants at the temperature of the experiment and the LO frequency at  $\tilde{q} = \pi/2r_0(111)$  for the neutron diffraction experiment, respectively.

The parameters thus determined have been used to calculate the phonon dispersion relations, the frequency spectra, and the variation of Debye tem-

TABLE I. Input data and parameters for the crystals.

| Crystal<br>Temp.      | KI <sup>b</sup><br>95 °K | Input data <sup>a</sup> |               |              |                |             | Parameters  |              |               |              |                |
|-----------------------|--------------------------|-------------------------|---------------|--------------|----------------|-------------|-------------|--------------|---------------|--------------|----------------|
|                       |                          | KBr<br>90 °K            | NaCl<br>80 °K | KCl<br>80 °K | NaBr<br>295 °K |             | KI<br>95 °K | KBr<br>90 °K | NaCl<br>80 °K | KCl<br>80 °K | NaBr<br>295 °K |
| Ref.                  |                          | 30                      | 34            | 36           | 37             | $\phi''$    | 1.9447      | 2.3093       | 2.8819        | 2.6551       | 2.3256         |
|                       |                          | 31                      | 35            | 35           | 38             |             |             |              |               |              |                |
|                       |                          | 32                      | 32            | 32           | 32             |             |             |              |               |              |                |
|                       |                          | 33                      | 33            | 33           | 27             | $\phi'/r_0$ | -0.2134     | -0.2332      | -0.2777       | -0.2728      | -0.2352        |
|                       |                          | 19                      | 25            | 26           | 27             |             |             |              |               |              |                |
| $\bar{C}_{11}$        | (0.325)                  | 0.438                   | 0.580         | 0.515        | 0.496          |             |             |              |               |              |                |
| $e_{11}$              |                          | 0.414                   | 0.548         | 0.491        | 0.357          | Y           | 2.999       | 3.6046       | 2.6263        | 3.5611       | 2.6203         |
| $\bar{C}_{12}$        | (0.032)                  | 0.050                   | 0.125         | 0.056        | 0.097          |             |             |              |               |              |                |
| $e_{12}$              |                          | 0.047                   | 0.119         | 0.053        | 0.434          | K           | 25.008      | 52.8978      | 45.3117       | 74.9831      | 31.7339        |
| $\bar{C}_{44}$        | (0.0369)                 | 0.057                   | 0.142         | 0.068        | 0.110          |             |             |              |               |              |                |
| $e_{44}$              |                          | 0.056                   | 0.141         | 0.069        | 0.106          |             |             |              |               |              |                |
| $r_0(\text{Å})$       | (3.504)                  | 3.278                   | 2.799         | 3.137        | 2.988          | P(1)        | -0.0803     | -0.1099      | -0.1088       | -0.0968      | -0.1575        |
| $\bar{r}_0(\text{Å})$ |                          | 3.267                   | 2.790         | 3.108        | 2.951          |             |             |              |               |              |                |
| $\epsilon_0$          | 4.66                     | 4.64                    | 5.53          | 4.53         | 6.28           | P(2)        | 0.0155      | 0.0518       | 0.1073        | 0.02116      | 0.0803         |
| $\epsilon_\infty$     | 2.69                     | 2.38                    | 2.31          | 2.09         | 2.62           |             |             |              |               |              |                |
| $\omega$              | 24.76                    | 27.43                   | 43.30         | 30.50        | 35.99          |             |             |              |               |              |                |
|                       |                          | (extd.)                 |               |              |                |             |             |              |               |              |                |

<sup>a</sup> $C_{11}$ , etc. and  $e_{11}$ , etc. are the harmonic and long-wave elastic constants, respectively. All elastic constants are in units of  $10^{12}$  dyn/cm<sup>2</sup>.  $\omega$  is in units of  $10^{12}$  s<sup>-1</sup>. References are arranged as follows: temperature derivative of the elastic constants, pressure derivative of the elastic constants, high-temperature linear thermal expansion coefficient, dielectric constants, and LO frequency [ $q = \pi/2r_0(111)$ ] for each crystal in the corresponding column.  $r$ ,  $\omega$ ,  $\epsilon_0$ , and  $\epsilon_\infty$  refer to values at the temperature of the neutron diffraction experiment for each crystal mentioned near the top of the table.  $\phi''$ ,  $\phi'/r_0$ ,  $k$ , P(1), and P(2) are in units of  $10^4$  dyn/cm.

<sup>b</sup>Values for this crystal refer to the temperature of the experiment.

perature for each crystal. In calculating the frequency distribution we have used the sample of 1000 points evenly distributed throughout  $\frac{1}{48}$  volume of the first Brillouin zone selected by Kellermann. The secular determinants in these directions have been solved in IBM 1130 and IBM 1620 computers. With a larger number of points in the mesh, the frequency distribution and the specific-heat calculation become more accurate. It is, however, expected that the mesh we use will give the general trend of the  $\Theta_D$ - $T$  curve fairly well. The Debye function is taken from a table by Harrison *et al.*<sup>13</sup> The input data and the values of the parameters for all the crystals are collected in Table I.

In the sections that follow we give the results for different crystals and discuss them separately.

### III. RESULTS AND DISCUSSION

#### A. KI

Figure 1(a) represents the DSM calculation of the dispersion relation in the symmetry directions, and compares the same with that of the simple shell model<sup>14</sup> (SSM) and the experimental observation.<sup>15</sup> We find that our calculation shows distinct improvement over the SSM. There is a calculation by Deo and Dayal<sup>14</sup> which shows some improvement for certain branches of the dispersion curves, but the over-all improvement is poorer than that

of the SSM. The dispersion relations for KI calculated on the model of Singh and Verma<sup>16</sup> show agreement similar to that of the present calculation. In the case of KI, we have not determined the parameters of the model according to the procedure of Sec. II. We have simply used the same set of input data as was used in the calculation of the SSM. Dolling *et al.*,<sup>15</sup> in addition to the SSM calculation, have used another model in which the SSM has been modified to include polarization of both ions, noncentral forces between nearest neighbors, and also central forces between next nearest neighbors. The ionic charge is also taken to be a variable. In this way there are 11 parameters which have been adjusted from the neutron-scattering results. They report excellent agreement between theory and experiment. However, the calculated high-frequency dielectric constant is about 10% too low. Furthermore the short-range polarizability of the positive ion turns out to be negative, indicating that the shell of the positive ion has a positive charge. This finding is in agreement with that of Cowley *et al.*<sup>17</sup> for NaI and KBr. That the agreement in the case of the SSM calculation is to a certain extent arbitrary has been demonstrated by Deo and Dayal for the case of KI.  $\phi''$  is, in general, determined from  $C_{11}$ . If this is determined from the compressibility for KI, the calculated frequencies are about 10% too low.

There is a calculation on the deformation dipole model (DDM)<sup>18</sup> which gives results similar to that of the SSM. From Fig. 3(a) we find that the order of agreement for low-temperature specific heat is similar for both the SSM and the DSM.

#### B. KBr

In the case of KBr, in addition to neutron diffraction measurement in the symmetry directions, an experiment has been done to obtain the frequencies in certain off-symmetry directions,<sup>19</sup> which directly provides a scope to test the validity of a model for directions other than the symmetry ones.

Figure 1(b) represents the experimental<sup>19</sup> points in the symmetry directions and the two theoretical curves calculated according to SSM<sup>17</sup> and DSM. There is a calculation by Karo and Hardy on DDM<sup>18</sup> which shows agreement similar to that of SSM. Figure 1(c) compares the results of SSM and DSM in the two off-symmetry directions with experiment. An examination of Figs. 1(b) and 1(c) shows that the agreement for DSM is quite satisfactory, and superior to that of SSM in both the symmetry and off-symmetry directions. In this case we find that, in fact, all the frequencies are reproduced almost within the range of experimental error. The calculations of BSM<sup>1</sup> and on the model due to Singh and Verma<sup>16</sup> also show similar agreement. The specific-heat calculation also shows that the agreement is closer for DSM. In this case the shell-model curve is calculated on an extended shell model,<sup>17</sup> where all the parameters are allowed to vary.

#### C. NaCl

Since Kellermann's pioneering work<sup>20</sup> on NaCl, a number of more complex models<sup>2,18,21-25</sup> have been proposed to describe the interaction of this solid. Of these models only Lundqvist's calculation<sup>2</sup> is based on first principles, but it could not properly explain the observations. In this section we consider first the DSM calculation of the phonon frequency of the crystal in comparison with experiment and with that due to other models.

The results of DSM and BSM calculations, together with the phonon dispersion relation of NaCl experimentally obtained by Raunio *et al.*<sup>26</sup> with the neutron diffraction technique, are presented in Fig. 1(d).

The agreement between theory and experiment is quite satisfactory for both the models except for a small discrepancy of the order of 4% in case of BSM for the LO branch in the [111]-direction zone boundary, and TO<sub>1</sub>-mode and TA-mode frequencies for large wave vectors in the [110] direction, the discrepancy in the latter cases being greater than the experimental error. In their ex-

periment on NaCl, Raunio *et al.*<sup>26</sup> claim that "except for higher frequencies the relative error is not greater than 0.5%." In this connection it is to be mentioned that in the BSM calculation an ionic charge  $Z = 1.0$  is used. In a later calculation by Nüsslein and Schröder using ionic charge  $Z = 0.9$ , the agreement is considerably poorer. This is, however, not always the case, as we shall see for other alkali halides.

There is a shell-model calculation by Caldwell and Klein<sup>25</sup> not shown in the figure which gives the main deviations to be confined to the following five areas: The [111] LO branch is up to 10% too high and also too flat; the LA branch at point  $L$  is about 10% low; the [110] LO branch has a peculiarity which is absent in experiment; the maxima in the LA branch in the [100] and [110] directions are 6% to 8% too low.

A six-parameter shell-model calculation by Namjoshi *et al.*<sup>21</sup> shows somewhat better agreement than that of the one just described. The DDM calculations<sup>18</sup> for NaCl show good agreement for the acoustic branches except near the zone boundaries, where the values are low by 5-8% for the [111] LA and [100] LA branches. For optical branches the agreement is significantly poorer, particularly near the zone boundary in the [110] direction. The characteristic discrepancy between theory and experiment for both SSM and DDM in the LO mode frequency in the [111] direction is also present but somewhat less pronounced than that of the shell model.

There are two other calculations<sup>22,24</sup> on NaCl which yield results more or less similar to DSM and BSM. In the results due to Melvin *et al.*<sup>22</sup> (a more generalized version of BSM), we find that there is a hump in the [100] LO frequency near the zone boundary, leading to a value of frequency nearly 10% greater than experiment, a characteristic discrepancy of their model. In the [110] direction the theoretical curve for TO<sub>1</sub> mode crosses the experimental curve at  $\vec{q} = (0.5, 0.5, 0)$  on the lower wave-vector side, the calculated results being about 4% below experiment, while on the higher wave-vector side it is up by 2% to 8%. In the [111] direction the LO mode and the TA frequency at (1.0, 0, 0) are nearly 5% off from experiment. Except for the frequencies mentioned above, the agreement is quite satisfactory. The calculations on the model of Singh and Verma<sup>24</sup> show better agreement with experiment than that of Melvin.<sup>22</sup> However, there are still certain discrepancies which are restricted to the following regions: In the [110] direction, the frequencies of the LO mode from  $\vec{q} = (0.2, 0.2, 0)$  to  $\vec{q} = (0.6, 0.6, 0)$  are about 5% above the experimental curve; the LO frequency in the [111]-direction zone boundary is about 4% greater than the experimental value;

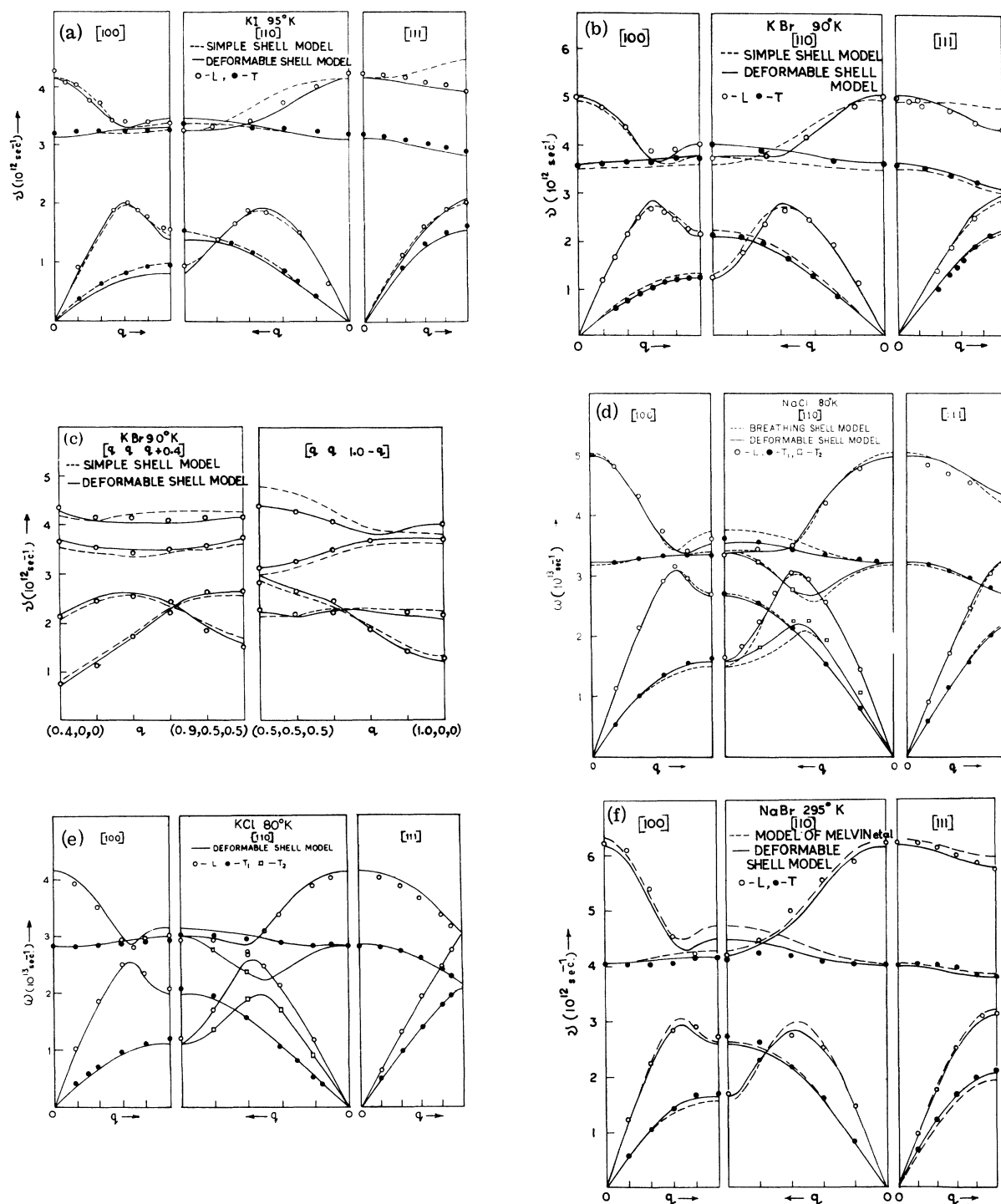


FIG. 1. Phonon dispersion curves for (a) KI, (b) and (c) KBr, (d) NaCl, (e) KCl, and (f) NaBr.

the LA-mode frequencies near the  $[111]$ -direction zone boundary are about 7% below experiment.

It is to be pointed out that the theoretical calculations referred to above, except for DSM, are made for  $0^\circ\text{K}$ , which will introduce a small deviation

from the experimental frequencies.

In the case of the present calculation the main discrepancy is confined to only one region, i. e., between  $\vec{q} = (0.2, 0.2, 0.2)$  and  $\vec{q} = (0.1, 0.1, 0.1)$  for LO-mode frequencies, the order of discrepancy

TABLE II. Comparison of experimental and theoretical frequencies at the point (1, 0, 0.5, 0) for NaCl (in units of  $10^{13} \text{ s}^{-1}$ ).

| Mode | Expt. (Ref. 26)   | DDM (Ref. 18)   | BSM (Ref. 23)              | BSM (Ref. 24)              | SM (Ref. 25)    | DSM              |
|------|-------------------|-----------------|----------------------------|----------------------------|-----------------|------------------|
|      | $\omega$ (80 °K)  | $\omega$ (0 °K) | $Z=1.0$<br>$\omega$ (0 °K) | $Z=0.9$<br>$\omega$ (0 °K) | $\omega$ (0 °K) | $\omega$ (80 °K) |
| TA   | $2.267 \pm 0.004$ | 2.278           | 2.28                       | 2.153                      | 2.20            | 2.27             |
| LA   | $2.65 \pm 0.01$   | 2.544           | 2.58                       | 2.63                       | 2.48            | 2.62             |
| TO   | $3.00 \pm 0.015$  | 2.993           | 2.96                       | 3.09                       | 3.25            | 2.98             |
| LO   | $3.51 \pm 0.015$  | 3.783           | 3.64                       | 3.415                      | 3.46            | 3.43             |

being nearly 4% higher than experiment. Considering all the calculations according to the different models, we notice that the best over-all agreement is obtained for DSM.

A close inspection of the above discussion reveals the fact that all the many-body interaction models considered here give significant improvement in agreement of varying degree between theory and experiment over SM and DDM. The difference in results between DSM, BSM, and the model of Singh and Verma might be partly due to slightly different values of the input data.

In Table II a comparison is made between several model results for frequencies in an off-symmetry direction, [1, 0, 0.5, 0], for which experimental results are available. Here also we find that DSM compared to others shows a better fit.

Next we have computed the specific-heat curve from the distribution function represented in Fig. 2(c). The DSM and BSM results together with experiment are shown in Fig. 3(c). Here also the agreement is quite fair. For the  $\Theta_D$ - $T$  curve the model of Singh and Verma<sup>24</sup> also shows satisfactory agreement. But as we know, the specific-heat calculation implies a gross averaging of the frequencies in which the finer details of a model are masked and hence the fit cannot be considered to be a distinct test for any model. However, for NaCl one distinct point to be noted is that the experimental specific-heat curve does not totally reproduce the characteristic dip at low temperature as in the case of other alkali halides. This peculiarity may be related to the large deviation from the Cauchy relation for NaCl. Of the Na halides, the Cauchy violation is largest for this crystal, which indicates the importance of many-body interaction. The theoretical curves considered in Fig. 3(c) reveal this feature, as both of them imply the types of many-body interaction not included in either SM or DDM.

#### D. KCl

In Fig. 1(e), the phonon frequencies experimentally determined by Raunio *et al.*<sup>27</sup> have been compared with the frequencies calculated at the same temperature on DSM. The agreement is

superior to that due to calculations on DDM<sup>18</sup> and SM<sup>21</sup> (not shown in figure), which show discrepancies characteristic of them.

There is a calculation on BSM<sup>27</sup> with an effective ionic charge of  $0.9e$  for which the discrepancies follow: the LA, LO, and TO frequencies for  $\vec{q} = (1, 0, 0, 0)$  are about 12%, 5%, and 5%, respectively, below experiment. For the present calculation the discrepancies for this value of wave vector are 6% below, 5% above, and within experimental error for the TO frequency. For other frequencies the predictions of the two models are similar. The calculations<sup>28</sup> on the model of Singh and Verma with 0 °K input data show better agreement for these frequencies.

In Table III, we compare DSM results with experiment<sup>27</sup> for the off-symmetry point (1, 0, 0.5, 0). For this point also we find the agreement to be satisfactory.

The specific-heat calculation, Fig. 3(d), also shows satisfactory agreement.

#### E. NaBr

Figure 1(f) compares the phonon frequencies calculated on DSM with the experimental observation<sup>29</sup> and another theoretical calculation on the model by Melvin *et al.*<sup>22</sup>

An examination of Fig. 1(f) shows that the order of agreement with experiment is more or less similar for both the models considered. For both the models in the [100]-direction zone boundary, the discrepancy is noticeable, and for the LO mode it is larger for the model of Melvin *et al.*<sup>29</sup> (12% above experiment). For the TA modes in all the three symmetry directions, the results predicted by the model of Melvin *et al.* are a few percent below experiment, while the DSM results are much closer to experiment. There is a DDM calculation by Karo and Hardy<sup>18</sup> which shows agreement characteristic of these models. The frequencies of the model with second-neighbor forces<sup>29</sup> show some improvement over those derived from DDM. There is another calculation on the model of Singh and Verma<sup>24</sup> which shows agreement similar to the present calculation.

Figure 3(e) compares the specific-heat calcula-

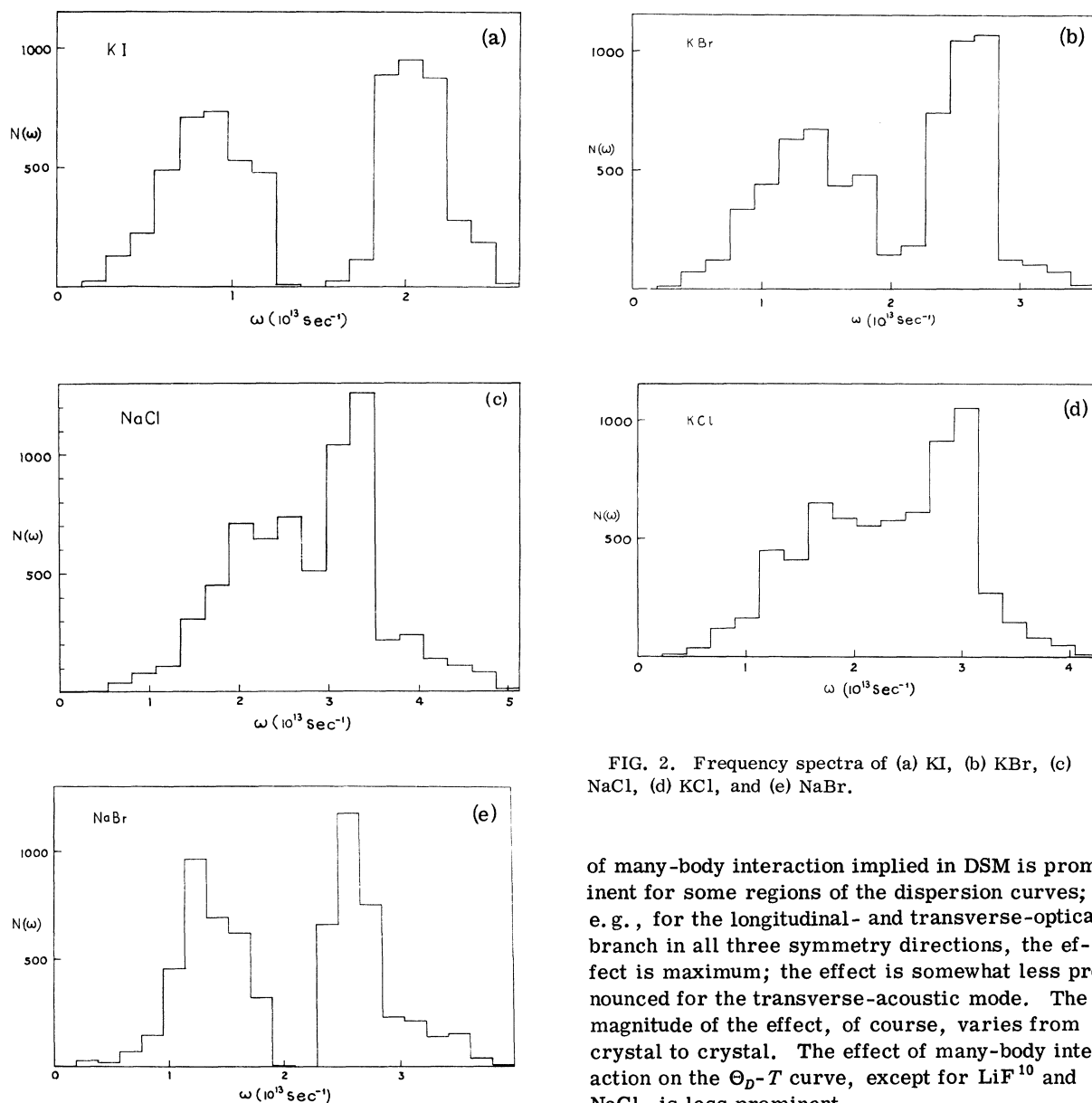


FIG. 2. Frequency spectra of (a) KI, (b) KBr, (c) NaCl, (d) KCl, and (e) NaBr.

of many-body interaction implied in DSM is prominent for some regions of the dispersion curves; e. g., for the longitudinal- and transverse-optical branch in all three symmetry directions, the effect is maximum; the effect is somewhat less pronounced for the transverse-acoustic mode. The magnitude of the effect, of course, varies from crystal to crystal. The effect of many-body interaction on the  $\Theta_D$ - $T$  curve, except for LiF<sup>10</sup> and NaCl, is less prominent.

BSM also includes the many-body interaction of a nature similar to that in DSM and gives good agreement in some cases. However, there are some essential differences between the two models as discussed in Ref. 5. As both the models fit the experiment by adjustment of some parameters, the differences tend to smooth out. At least from the study of the dispersion curves and  $\Theta_D$ - $T$  curves it is difficult to ascertain which model fits the experiment better. Moreover, in most applications of BSM, both ions are taken as polarizable and second-neighbor and noncentral interactions are also included in addition to the breathing effect. We have in our application consistently used only the negative-ion polarizable model and, except for the case of LiF, neglected the second-neighbor

tion on DSM with that calculated on the model by Melvin *et al.*<sup>29</sup>

The input data for the crystals considered above are taken from Refs. 19, 25-27, and 30-38.

#### IV. CONCLUSION

A survey of the results of the application of the deformable-shell model considered here clearly indicates that the agreement between theory and experiment both for the dispersion relation and low-temperature specific heat of the alkali halides is fairly good and suggests a definite improvement over both SM and DDM. It is noted that the effect

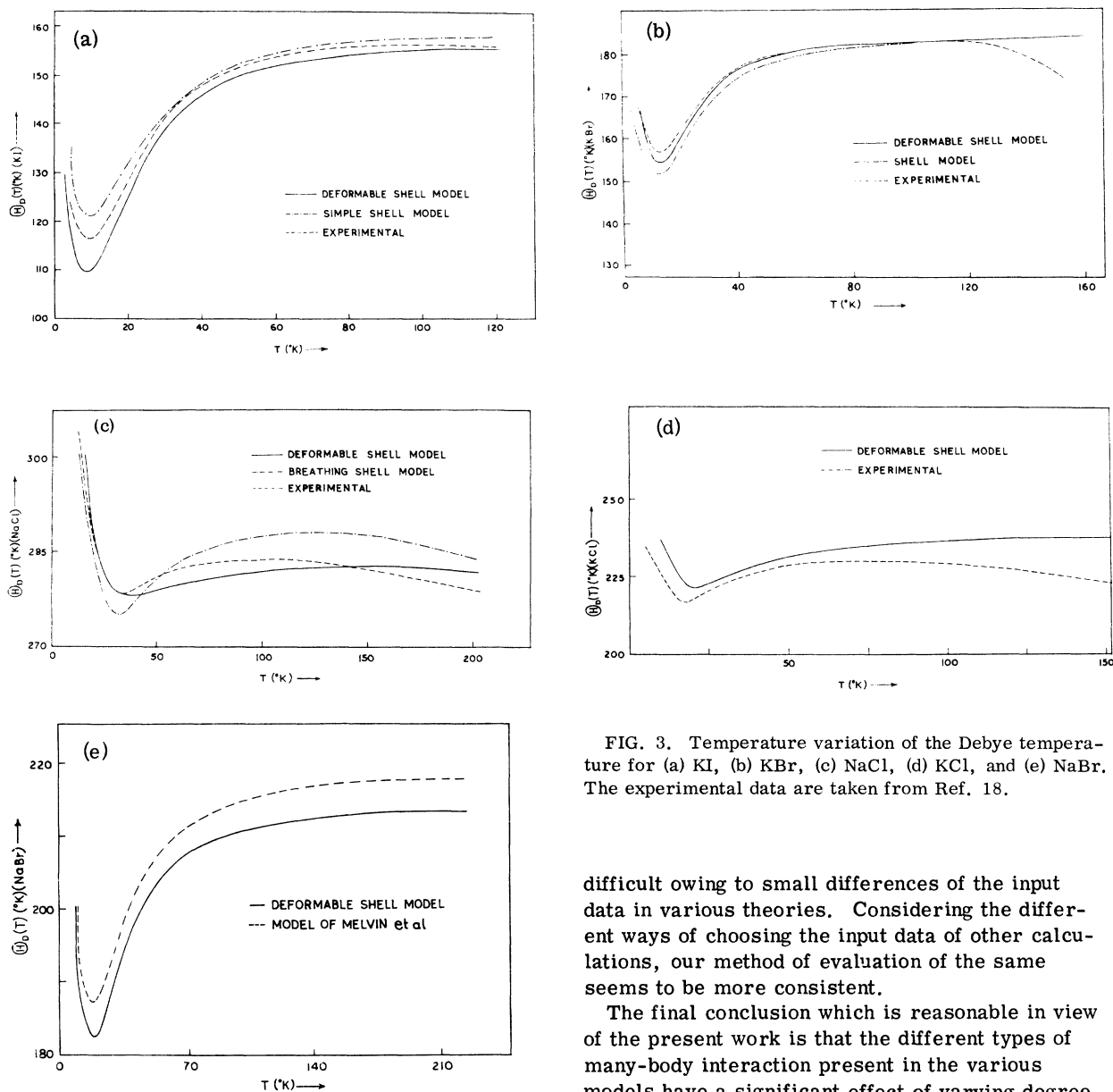


FIG. 3. Temperature variation of the Debye temperature for (a) KI, (b) KBr, (c) NaCl, (d) KCl, and (e) NaBr. The experimental data are taken from Ref. 18.

difficult owing to small differences of the input data in various theories. Considering the different ways of choosing the input data of other calculations, our method of evaluation of the same seems to be more consistent.

The final conclusion which is reasonable in view of the present work is that the different types of many-body interaction present in the various models have a significant effect of varying degree on the phonon frequencies of the alkali halides and so far as the dynamic properties of the crystals considered in the present investigation are concerned, the order of variation is not pronounced enough to draw any definite conclusion about the superiority of any particular model. However,

overlap effect. Because of these differences, a comparative study of agreement with experiment for these two models becomes difficult.

The other model<sup>3</sup> which also includes the many-body interaction proposed by Lundqvist<sup>2</sup> is definitely different in principle from both BSM and DSM. But when a calculation is made by adjustment of parameters the differences cease to be prominent, because the dominant contribution to dynamical matrix<sup>5</sup> from the many-body interaction has the same formal structure as in DSM and BSM.

Strict comparison between different many-body-interaction-model results is further rendered

TABLE III. Comparison of experimental and theoretical frequencies at the point (1, 0, 0.5, 0) for KCl (in units of  $10^{13}$  s<sup>-1</sup>).

| Mode            | LO              | TO              | LA              | TA              |
|-----------------|-----------------|-----------------|-----------------|-----------------|
| Expt.           |                 |                 |                 |                 |
| $\omega$ (80°K) | $2.96 \pm 0.02$ | $2.39 \pm 0.02$ | $1.65 \pm 0.02$ | $1.65 \pm 0.02$ |
| DSM             |                 |                 |                 |                 |
| $\omega$ (80°K) | 3.11            | 2.47            | 1.63            | 1.63            |



for certain crystals, for example NaI (not discussed in this work), it is noted that the order of difference between DSM and Lundqvist's model calculations<sup>4,24</sup> for certain frequencies ( $\omega$ ) is as high as 15%, the agreement with experiment being better for DSM; we think this cannot be explained in

terms of variation of the input data alone.

#### ACKNOWLEDGMENT

Our grateful thanks are due to Dr. P. Banerjee for his valuable help in connection with the computation work.

- 
- <sup>1</sup>U. Schröder, *Solid State Commun.* **4**, 347 (1966).  
<sup>2</sup>S. O. Lundqvist, *Ark. Fys.* **12**, 263 (1957).  
<sup>3</sup>R. K. Singh and M. P. Verma, *Phys. Status Solidi* **33**, 769 (1969); *Phys. Status Solidi* **36**, 335 (1969).  
<sup>4</sup>A. N. Basu and S. Sengupta, *Phys. Status Solidi* **29**, 367 (1968).  
<sup>5</sup>A. N. Basu, D. Roy, and S. Sengupta (unpublished).  
<sup>6</sup>A. K. Sarkar and S. Sengupta, *Solid State Commun.* **7**, 135 (1969); *Phys. Status Solidi* **35**, 499 (1969).  
<sup>7</sup>A. K. Sarkar, in *Proceedings of the Nuclear Physics and Solid State Physics Symposium, Roorkee, India, 1969* (unpublished).  
<sup>8</sup>S. Paul, A. K. Sarkar, and S. Sengupta, *Phys. Status Solidi* **54**, 321 (1972).  
<sup>9</sup>D. Roy, A. N. Basu, and S. Sengupta, *Phys. Rev. B* **5**, 4987 (1972).  
<sup>10</sup>A. N. Basu and S. Sengupta, *J. Phys. C* **5**, 1158 (1972).  
<sup>11</sup>A. D. B. Woods, W. Cochran, and B. N. Brockhouse, *Phys. Rev.* **119**, 980 (1960).  
<sup>12</sup>D. Roy, A. N. Basu, and S. Sengupta, *Phys. Status Solidi* **35**, 499 (1969).  
<sup>13</sup>Don E. Harrison, Jr. and John R. Neighbours, *Research Report No. 49, United States Naval Postgraduate School, 1964* (unpublished).  
<sup>14</sup>R. G. Deo and B. Dayal, *Can. J. Phys.* **45**, 1885 (1967).  
<sup>15</sup>G. Dolling, R. A. Cowley, C. Schittenhelm, and I. M. Thorson, *Phys. Rev.* **147**, 577 (1966).  
<sup>16</sup>R. K. Singh and M. P. Verma, *Phys. Status Solidi* **36**, 335 (1969).  
<sup>17</sup>R. A. Cowley and W. Cochran, *Phys. Rev.* **131**, 1030 (1963).  
<sup>18</sup>A. M. Karo and J. R. Hardy, *University of California Radiation Laboratory Report No. 6893, 1962* (unpublished).  
<sup>19</sup>A. D. B. Woods, B. N. Brockhouse, and R. A. Cowley, *Phys. Rev.* **131**, 1025 (1963).  
<sup>20</sup>E. W. Kellermann, *Philos. Trans. R. Soc. Lond.* **238**, 513 (1940); *Proc. R. Soc. A* **178**, 17 (1941).  
<sup>21</sup>K. V. Namjoshi, S. S. Mitra, and J. F. Vetelino, *Phys. Rev. B* **3**, 4398 (1971).  
<sup>22</sup>J. S. Melvin, J. D. Pirie, and T. Smith, *Phys. Rev.* **175**, 1082 (1968).  
<sup>23</sup>V. Nüsslein and U. Schröder, *Phys. Status Solidi* **21**, 309 (1967).  
<sup>24</sup>R. K. Singh and M. P. Verma, *Phys. Rev. B* **2**, 4288 (1970).  
<sup>25</sup>R. F. Caldwell and M. V. Klein, *Phys. Rev.* **158**, 851 (1967).  
<sup>26</sup>G. Raunio, L. Almquist, and R. Stedman, *Phys. Rev.* **178**, 1496 (1969).  
<sup>27</sup>G. Raunio and L. Almquist, *Phys. Status Solidi* **33**, 209 (1969).  
<sup>28</sup>R. K. Singh and M. P. Verma, *Phys. Status Solidi* **38**, 851 (1970).  
<sup>29</sup>J. S. Reid, T. Smith, and W. J. L. Buyers, *Phys. Rev. B* **1**, 1833 (1970).  
<sup>30</sup>S. P. Nikanorov and A. V. Stepanov, *Zh. Eksp. Teor. Fiz.* **37**, 1814 (1959) [*Sov. Phys.-JETP* **10**, 1280 (1960)].  
<sup>31</sup>G. R. Barsch and Z. P. Chang, *Phys. Status Solidi* **19**, 139 (1967).  
<sup>32</sup>J. G. Collins and G. K. White, in *Progress in Low Temperature Physics*, edited by G. J. Gorter (North-Holland, Amsterdam, 1964), p. 450.  
<sup>33</sup>R. P. Lowndes and D. H. Martin, *Proc. R. Soc. A* **308**, 473 (1969).  
<sup>34</sup>A. V. Stepanov and I. M. Eidus, *Zh. Eksp. Teor. Fiz.* **29**, 669 (1955) [*Sov. Phys.-JETP* **2**, 377 (1956)].  
<sup>35</sup>R. A. Bartels and D. E. Schuele, *J. Phys. Chem. Solids* **26**, 537 (1965).  
<sup>36</sup>G. Leibfried and W. Ludwig, *Solid State Physics*, edited by F. Seitz and D. Turnbull (Academic, New York, 1961), Vol. 12, p. 368.  
<sup>37</sup>J. T. Lewis, A. Lehoczy, and C. V. Briscoe, *Phys. Rev.* **161**, 877 (1967).  
<sup>38</sup>K. M. Koliwad, P. B. Ghate, and A. L. Ruoff, *Phys. Status Solidi* **21**, 507 (1967).